

Growth and spectroscopic characterization of organic polymer-stabilized CdS nanoparticles

YU. M. AZHNIUK^{a*}, V. M. DZHAGAN^a, YU. I. HUTYCH, A. E. RAEVSKAYA^b, A. L. STROYUK^b,
S. YA. KUCHMIY^b, M. YA. VALAKH^a, D. R. T. ZAHN^c

Institute of Electron Physics, Ukr. Nat. Acad. Sci., Universytetska Str. 21, Uzhhorod 88017, Ukraine

^aInstitute of Semiconductor Physics, Ukr. Nat. Acad. Sci., Prospect Nauky 41, Kyiv 03028, Ukraine

^bInstitute of Physical Chemistry, Ukr. Nat. Acad. Sci., Prospect Nauky 31, Kyiv 03028, Ukraine

^cChemnitz University of Technology, Semiconductor Physics, D-09107 Chemnitz, Germany

CdS nanoparticles were obtained from aqueous solutions at relatively mild conditions and embedded into a matrix of organic polymer (gelatin, polyacrylamide, polyvinyl alcohol). Spectroscopic techniques (absorption, photoluminescence, Raman scattering) are used for their characterization. Raman spectra of the organic-polymer stabilized CdS nanoparticles are discussed taking into account phonon confinement and scattering by surface phonons. The dependence of surface phonon frequency in CdS nanoparticles on the Raman excitation wavelength is observed to be much stronger than on the host medium type.

(Received September 30, 2008; accepted March 19, 2009)

Keywords: Semiconductor nanoparticles, optical absorption, photoluminescence, Raman scattering

1. Introduction

Within the past two decades II-VI semiconductor nanoparticles have become an object of particular research interest due to a number of unique size-dependent optical properties that have already found numerous applications (e. g. [1–8]). A variety of techniques have been elaborated to obtain CdS nanoparticles of various size and topology to tailor the expected physical characteristics, especially luminescence, whose spectral position can be effectively varied across a broad spectral range (e. g. [1–3, 5, 6, 9–22]), the methods of colloidal synthesis being the most appropriate for the obtaining of CdS nanoparticles of good optical quality and small size dispersion. Nanoparticles of cadmium sulphide and composite core/shell nanostructures based on CdS have been extensively studied *e.g.* as photocatalysts, as potential active media for optical and optoelectronic devices, solar cells, memory elements, as fluorescent labels in biophysical experiments and other applications [1–5, 7, 16, 18, 23–27]. Hence, the interest in the growth and characterization of CdS nanoparticles as well as in their extended optical studies is driven by both fundamental and applied aspects of science.

Here we report on the results of synthesis of CdS nanoparticles with good optical characteristics at comparatively mild conditions from aqueous solutions, stabilized by organic polymeric species (polyvinyl alcohol, polyacrylamide, gelatin) and their characterization by optical absorption, photoluminescence, and Raman scattering.

2. Experimental

The technique for obtaining CdS nanoparticles in organic polymer media was basically similar to that reported in refs. [28, 29]. For the synthesis of gelatin-stabilized CdS nanoparticles 17.5 ml 0.2 M CdSO₄ solution were mixed with 7.5 ml 15 w% gelatin solution. Separately 17.5 ml 0.2 M Na₂S solution were also mixed with 7.5 ml 15 w% gelatin solution. Experiments with various amounts of excessive Na₂S in the reaction mixture were performed in order to study the effect of excessive Na₂S concentration on the obtained nanoparticle size. The two polymer-containing solutions were mixed at intense stirring to produce 50 ml of lemon-yellow colloidal CdS solution containing 4.5 w% gelatin and 0.07 M CdS. This solution was then cooled to 5–7 °C to produce a gel. To remove residual salts from the as-synthesized CdS colloids the gels were chopped into pieces and immersed in double-distilled water where they were kept for 3–4 days at 5–7 °C, the water being changed every 12 h.

The purified gelatin gel with CdS nanoparticles was heated to 40–50 °C to obtain viscous colloidal solution. Following a typical procedure, the viscous (10–15 % gelatin) colloidal CdS solution was deposited onto a glass plate which previously had been treated successively with concentrated H₂O₂ and H₂SO₄. Plates with as-deposited humid gelatin films were dried at 15–20°C in the dark at natural ventilation for 3–5 days.

In order to obtain CdS nanoparticles in polyacrylamide (PAA), 1 g acrylamide were added to 6 ml gelatin-stabilized CdS colloid. The resulting solution was exposed to illumination with $\lambda=365$ nm for 2 h for the photochemical formation of PAA. The procedure resulted in a colloidal solution with CdS concentration of 5×10^{-3} M in 20% PAA solution. Then it was dried on a glass plate to produce a film.

For obtaining CdS nanoparticles in polyvinyl alcohol (PVA), CdS nanoparticles were synthesized from CdSO₄ and Na₂S at 5 °C in 3% PVA. Then 5 ml of 15% PVA were added to 5 ml of the CdS colloid and the film was deposited.

The optical absorption and photoluminescence (PL) spectra of the polymer-stabilized CdS nanoparticles were obtained using a LOMO MDR-23 monochromator with a FEU-100 phototube, the instrumental width not exceeding 0.5 nm. The PL excitation was provided by a He–Cd laser (441.6 nm). Raman spectra were measured using a Dilor XY 800 triple monochromator with a CCD-camera, Ar⁺ laser ($\lambda_{\text{exc}}=457.9, 476.5,$ and 488.0 nm) being used for excitation. The resolution in the Raman spectra was better than 3 cm^{-1} . All measurements were performed at room temperature.

3. Results and discussion

Optical absorption and PL spectra of CdS nanoparticles embedded in gelatin, are shown in Fig. 1 for different excessive concentration of Na₂S in the reaction mixture. In the absorption spectra the confinement-related features are observed as shoulders rather than distinct maxima, what is rather typical when the nanoparticle size dispersion exceeds the value of about 15 %. Therefore, in order to determine the confinement-related absorption maxima position, we used, similarly to [30], the spectra of the observed absorption increment over the $\alpha^2 \sim h\nu$ dependence, typical for allowed direct transitions in semiconductors. Thus determined absorption maxima positions E_1 , indicated in Fig. 1, enabled us to estimate the average nanoparticle diameter d , following the known $E_1(d)$ dependence [31]. We based our estimations on the phenomenological dependence [31], as it was built on the base of transmission electron microscopy (TEM) measurements and showed a good agreement with the data of other authors (the references therein). The effective-mass approximation (EMA) [32], on the other hand, results in a considerable deviation from the experimental data for small nanoparticles. A potential-morphing method for nanoparticle size evaluation from the absorption spectra, based on the EMA [33], is not quite convincing since the choice of the confinement potential for charge carriers in CdS nanoparticles, depending on the host matrix band-gap energy, does not seem to be justified. By comparing the results of [32] and [33] with each other and with the experimental data, one can see that the effect of the confinement potential (i. e., of the host matrix, as follows from [33]) is revealed only for the CdS

nanoparticle radius below 1.5 nm while for larger nanoparticles a good agreement is observed.

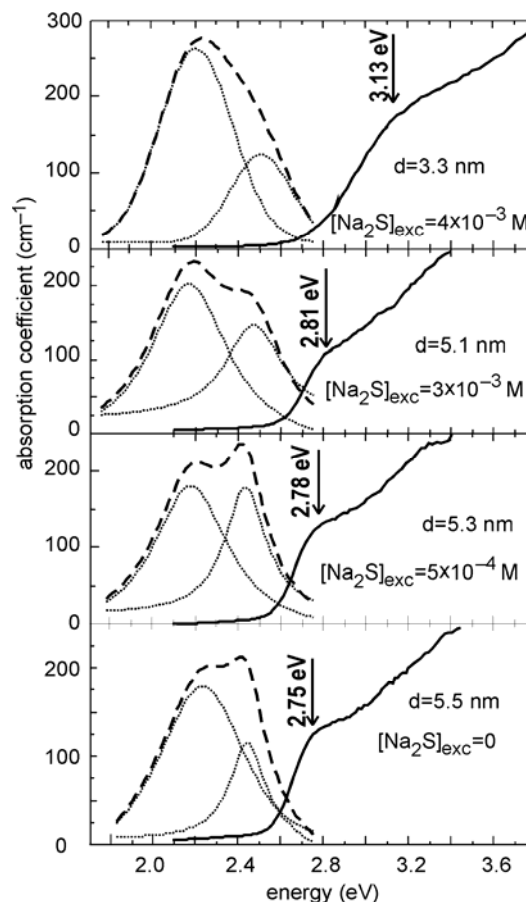


Fig. 1. Optical absorption (solid lines) and PL (dashed lines) spectra of gelatin-embedded CdS nanoparticles for different concentrations of excessive Na₂S; $[\text{CdCl}_2] = 5 \times 10^{-3}$ M. Dotted lines represent the PL spectrum decomposition into two emission bands.

As seen from the absorption spectra in Fig. 1, when equal concentrations of CdCl₂ and Na₂S react in the presence of gelatin, nanoparticles with average size 5.5 nm are obtained. A gradual increase of Na₂S content in the reaction mixture leads to a gradual shift of the absorption edge and the confinement-related features towards higher energies, revealing the nanoparticle size decrease down to 3.3 nm when the Na₂S concentration is almost twice that of CdCl₂, which is an evidence for the inhibition of exchange reaction resulting in the nanoparticle formation. It is worth noticing that at the reaction mixture heating an opposite effect is revealed –the average nanoparticle size increases what is clearly seen from the long-wavelength shift of the absorption edge and the confinement-related maximum (Fig. 2).

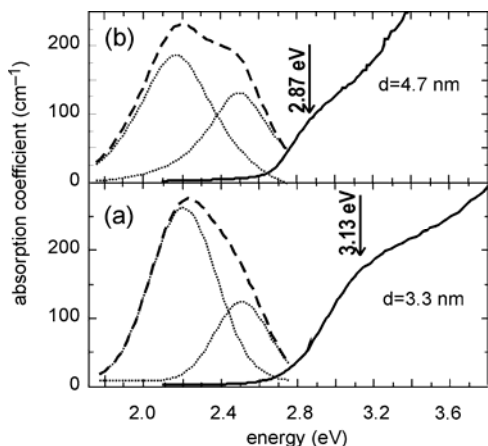


Fig. 2. Optical absorption (solid lines) and PL (dashed lines) spectra of CdS nanoparticles encapsulated in gelatin: (a) without and (b) with additional heating during 40 min at 80 °C; $[CdCl_2] = 5 \times 10^{-3}$ M, $[Na_2S] = 9 \times 10^{-3}$ M. Dotted lines represent the observed luminescence spectrum simulation by the long-wavelength and short-wavelength bands.

Optical absorption spectra of CdS nanoparticles stabilized in organic polymer matrices of PVA and PAA, are shown in Fig. 3 (a) and (b), respectively, in comparison with those of gelatin-encapsulated CdS nanoparticles of approximately the same average size. For the nanoparticle size range under consideration the matrix does not affect the relationship between the nanoparticle size and the energy of the first absorption maximum. It is clearly seen that for both PVA- and PAA-stabilized CdS nanoparticles the absorption edge shape is less steep and the confinement-related maxima are less pronounced than for the gelatin-encapsulated nanoparticles of the same size (Fig. 3). This can be explained by better size dispersion provided by the technique of nanoparticle stabilizing in gelatin in comparison with PVA and PAA.

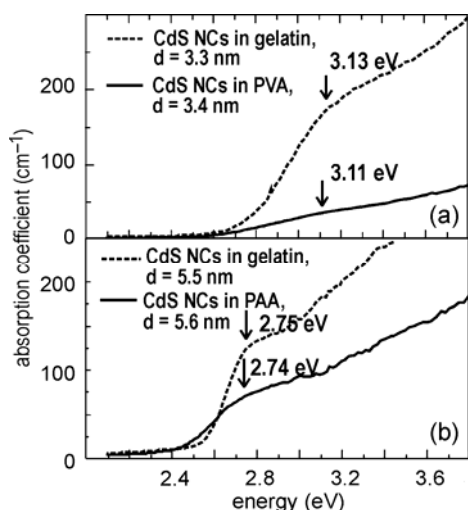


Fig. 3. Comparison of optical absorption spectra of CdS nanoparticles of practically the same size embedded in: (a) gelatin and PVA; (b) gelatin and PAA.

The PL spectra of CdS nanoparticles (Fig. 1) clearly reveal the presence of two emission bands. A near-bandgap emission peak is often explained in a "dark exciton" model, taking into account the exciton state fine structure due to the structural anisotropy and electron-hole exchange interaction [32]. An alternative explanation, especially regarding the PL band width, is based on exciton-acoustic phonon scattering [33]. The observed near-bandgap luminescence maximum energy position increases with the nanocrystal size decrease. The Stokes shift (the energy difference between the first absorption maximum and the near-bandgap emission peak) in the gelatin-embedded CdS nanoparticles considerably increases with the average size decrease what is typical for II-VI nanocrystals [34, 35], both the "dark exciton" and exciton-acoustic phonon coupling models having been invoked for the explanation [35]. However, in our case the excitonic origin of the higher-energy PL band seems somewhat doubtful due to its large halfwidth and large Stokes shift. Besides, the position of this band depends on the size decrease with the sulphur agent excess and does not depend on the size increase due to the sample heating (Fig. 1). This can support the idea of the band being defect-related. Evidently, the discussion of the band nature requires further studies.

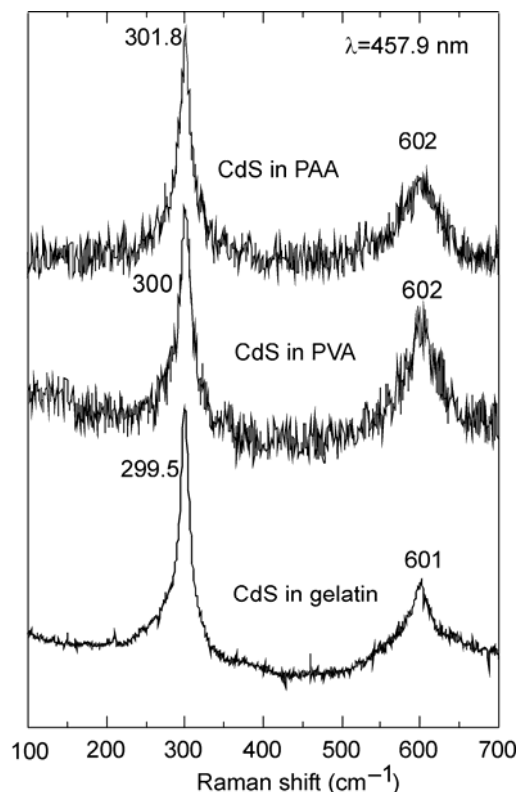


Fig. 4. Raman scattering spectra of CdS nanoparticles embedded in gelatin, PVA, and PAA.

A broader band, significantly shifted towards lower energies, is attributed to recombination mediated by surface states, in particular S^- traps or V^{2+} anion vacancies [10, 18]. Its independence on the nanoparticle size is consistent with the judgement of the band being related to sulphur vacancies [36].

Raman scattering spectra of CdS nanoparticles, embedded in three different organic polymer matrices, measured at the excitation by 457.9 nm laser line, are shown in Fig. 4. All the spectra are very much similar, containing a CdS LO phonon band centred near 300 cm^{-1} and a considerably broader band near 600 cm^{-1} related to a second-order scattering process with the participation of two LO phonons. The corresponding phonon frequency values are somewhat below those reported for single crystals [37]. This difference, as well as the observed asymmetric shape of the LO phonon band with a more pronounced low-frequency wing are related to the factors, affecting Raman spectra of nanocrystals, in particular, phonon confinement and surface phonon scattering [38–42 and references therein].

In nanocrystals with the size below about 10 nm, a phonon can no longer be described by a planar wave, but as a wave packet whose spatial dimensions are comparable to the crystalline size [43]. Thus, a spread or uncertainty in the wave vector q is introduced, which increases with the grain size decrease because the wave packet becomes more localized in space. As LO phonon dispersion curves in semiconductors (in particular, in CdS [44]) are not flat, but have a maximum at the Brillouin zone centre, the contribution of the phonons with $q \neq 0$ increases Raman scattering intensity below the $q=0$ LO phonon frequency, what should result in the band broadening and asymmetry with a more pronounced low-frequency wing as well as a slight frequency decrease [38–42]. Therefore, the observed LO phonon frequency ($\omega_{LO}=300\text{--}302\text{ cm}^{-1}$) is below the bulk CdS crystal value ($\omega_{LO}=305\text{ cm}^{-1}$ [37]). This is consistent with the data for CdS nanoparticles embedded in organic polymer ($\omega_{LO}=302\text{ cm}^{-1}$ [45]) as well as for nanopowders of different crystal shape obtained by chemical route ($\omega_{LO}=300\text{--}301\text{ cm}^{-1}$ [46–48]), CdS nanowires grown by chemical-vapour deposition ($\omega_{LO}=301\text{ cm}^{-1}$ [49]), and CdS nanotubes in PAA ($\omega_{LO}=301\text{ cm}^{-1}$ [50]). A quite unexpectedly low value of CdS-like LO phonon frequency (280 cm^{-1}) is reported for CdS nanoparticles in a mesoporous copolymer template [51], however, the authors fail to give any reasonable explanation for such an observation. Meanwhile, the Raman spectra of CdS nanoparticles of about the same size range, grown in SiO_2 [52] or borosilicate glass [53–55] matrix, exhibit LO phonon scattering at 305 cm^{-1} . This discrepancy is related to the compressive strain arising for CdS nanoparticles in silicate glass due to the matrix pressure, slightly increasing the phonon frequency [56]. The value of $\omega_{LO}=305\text{ cm}^{-1}$, reported for CdS nanocrystals, grown on a glass surface [57], can be also attributed to strain as well as the larger nanocrystal size and non-stoichiometry, mentioned by the authors.

Still the observed LO phonon frequency of CdS nanoparticles in organic media is lower than the value predicted by the calculations, taking into account the phonon confinement in the approach of Campbell and

Fauchet [40, 43]. Besides, the LO phonon frequency shift due to the phonon confinement should be dependent of the nanoparticle size, while we did not observe any noticeable dependence. Note that Raman studies of CdS nanoparticles embedded in another organic polymer Nafion [45] have also shown no size dependence of the LO phonon frequency, though the nanocrystal diameter was decreased from 6 to 1.6 nm. The authors of Ref. [45] explained this by a compensation of the confinement-related downward shift of the LO phonon frequency and the compressive strain-related frequency increase. However, such explanation should imply a noticeable size dependence of the host matrix pressure on the nanocrystals. Meanwhile, no such dependence has been observed in the studies of the external pressure effect on the optical spectra of glass-embedded $\text{CdS}_{1-x}\text{Se}_x$ nanocrystals [58], neither it is reported elsewhere. In our opinion, the major reason for the observed size-independent LO phonon frequency in polymer-embedded CdS nanoparticles is related to the Raman resonance and the nanoparticle size dispersion within the ensemble [42, 59].

Since nanoparticles comprise only a small fraction (of the order of 1 %) of the sample scattering volume, resonant conditions are required in order to obtain sufficient Raman signal. For a given excitation laser wavelength the average Raman cross section per unit of solid angle Ω_s and unit frequency ω_s of the nanoparticles with a certain size distribution is given by [60]

$$\left\langle \frac{d^2\sigma}{d\omega_s d\Omega_s} \right\rangle = \int \frac{d^2\sigma}{d\omega_s d\Omega_s}(R)F(R)dR \quad (1)$$

where $F(R)$ is the nanoparticle distribution function in radius R . According to the function $F(R)$, the resonant conditions select for the Raman spectra a set of nanoparticles with radii $\{R_i\}$ [60]. These particular dots give the main contribution to the spectrum selecting those phonon modes with frequencies ω_{n_p} ($n_p=0, R_i$) (the modes are labeled by a set of integer numbers $p \equiv [n_p, l_p, m_p]$ where l_p and m_p are related to their symmetry properties and angular momentum). Hence, an asymmetric and broadening Raman lineshape is obtained due to the several optical vibrations with different quantum number n_p participating in the process. The relative contribution of the confined phonon and excitonic states to the cross section depends strongly on the excited laser energy, the excitonic oscillator strength, and the electron-phonon Fröhlich interaction. In particular, when the incoming or scattered light select nanoparticles with small radii, the phonon line shape will be more asymmetric. For a given phonon mode in a nanoparticle with radius R the frequency uncertainty $\delta\omega_{n_p}$ can be evaluated as [60]

$$\frac{\delta\omega_{n_p}}{\omega_{n_p}} = \frac{(\beta_L\mu_n)^2}{(\omega_{LO}R)^2 - (\beta_L\mu_n)^2} \frac{\delta R}{R} \quad (2)$$

where β_L is a parameter characterizing the bulk LO phonon dispersion, ω_{LO} is the LO phonon frequency, μ_n is the n -th zero of the spherical Bessel function J_l , and $\delta R \geq |R - R_i|$.

Hence, the greater contribution to the resonant Raman spectrum will be made by those nanoparticles of the ensemble, for which the excitonic transition energy coincides with the energy of the exciting (incoming resonance) or scattered (outgoing resonance) light. Therefore, in order to trace the size-dependent shift of LO phonon frequency in nanoparticles, resonant Raman measurements at a series of excitation wavelengths are required. Detailed experimental and theoretical studies of disorder effects, related to nanoparticle size and shape dispersion within the ensemble of CdS nanocrystals in a dielectric matrix, were carried out in [52]. It should be noted that a resonant dependence of LO phonon frequency was also reported for CdS nanoparticles synthesized in mesoporous aluminosilicates [61]; however, their quantitative data are hardly reliable since they report on the observed bulk CdS LO phonon frequency of 299 cm^{-1} which strongly differs from the well-known value ($\omega_{LO} = 305\text{--}307 \text{ cm}^{-1}$ [37, 62 and references therein]).

Another factor, affecting the Raman spectra of nanoparticles, is scattering by surface phonons. It is known [63] that in a set of nanospheres of diameter d , embedded in a medium with a real, frequency independent dielectric constant ϵ_m , additional surface-related modes should be observed at the frequencies $\omega_{SO,l}$ between those for LO and TO phonons of the nanosphere material ω_{LO} and ω_{TO} , corresponding to

$$\epsilon_{\omega_j} \left[1 + \frac{\omega_{LO}^2 - \omega_{TO}^2}{\omega_{TO}^2 - \omega_{SO}^2} \right] = \frac{(l+1)}{l} \epsilon_m \quad (3)$$

where $l=1, 2, 3, \dots$. The intensity of these modes in nanocrystals decays with increasing distance from the surface of the sphere as $1/r^{l-1}$, at the exception of a so-called Fröhlich mode for $l=1$ which has constant amplitude over the whole volume of the sphere [63]. Evidently, the contribution of the surface phonons in the Raman spectrum becomes increasingly important with the increase of surface-to-volume ratio [38–40].

Being considerably broader than the LO phonon bands, surface phonons in nanoparticles are usually not observed as separate spectral maxima, but rather as a shoulder or asymmetry at the low-frequency side of the LO phonon peak. Attribution of a narrow peak at 276 cm^{-1} in PVA-embedded CdS nanoparticles in an earlier study [64] to surface phonons is hardly convincing since it is considerably narrower than the LO phonon. None of the subsequent studies has reported on such a narrow peak.

Comparison of surface phonon characteristics for CdS nanoparticles embedded in different organic media seemed interesting in view of the expected effect of the differences in the formation of the interface between the nanoparticles and the host medium on the CdS surface phonon

parameters. However, the observed situation appeared somewhat more complicated.

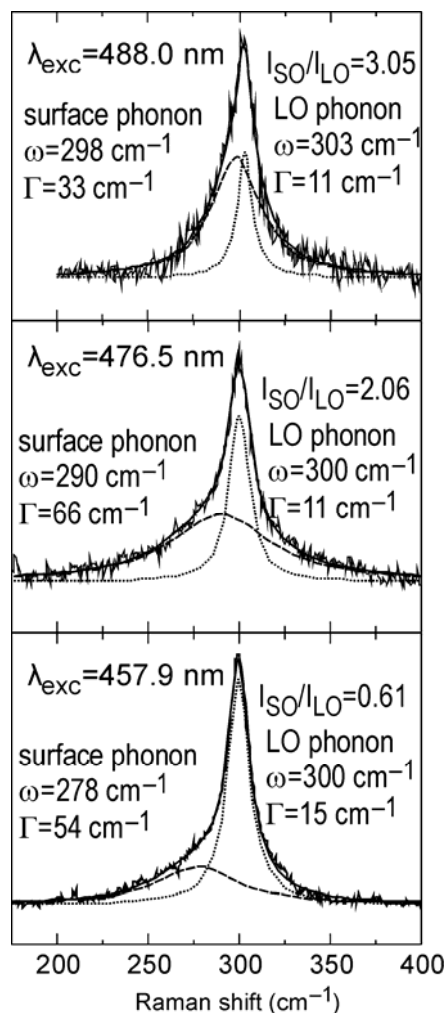


Fig. 5. First-order Raman scattering spectra of CdS nanoparticles embedded in gelatin ($d=5.5 \text{ nm}$), measured at different excitation wavelengths. The contribution of LO phonons (dotted lines) and surface phonons (dashed lines) is shown.

Contributions of LO phonons and surface phonons to the Raman spectra of CdS nanoparticles in gelatin, measured at different excitation wavelengths, are shown in Fig. 5. A strong dependence of the surface phonon parameters in gelatin-embedded CdS nanoparticles on the Raman resonance conditions is clearly seen. With the Raman excitation energy increase, corresponding to the wavelength variation from 457.9 to 488.0 nm, the surface phonon frequency shift from 278 to 298 cm^{-1} is observed along with a substantial variation of the surface phonon bandwidth and a drastical (by factor of 5) decrease of the surface-to-LO phonon intensity ratio. A similar situation is observed for CdS nanoparticles embedded in PAA. Unfortunately, for PVA-stabilized CdS nanocrystals (where the nanoparticle concentration in the film was

smaller than for those in gelatin and PAA) Raman signal could be detected only for the excitation by 457.9 nm laser light. The surface phonon characteristics, obtained from the Raman spectra of CdS nanoparticles in different organic host media, are summarized in Table 1.

Table 1. Surface phonon frequencies ω_{SO} and halfwidths Γ_{SO} , observed for CdS nanoparticles in different organic polymer matrix at different Raman excitation wavelengths (all values in cm^{-1})

Host medium	$\lambda_{\text{exc}} = 457.9 \text{ nm}$		$\lambda_{\text{exc}} = 476.5 \text{ nm}$		$\lambda_{\text{exc}} = 488 \text{ nm}$	
	ω_{SO}	Γ_{SO}	ω_{SO}	Γ_{SO}	ω_{SO}	Γ_{SO}
gelatin	278	54	290	66	298	33
PAA	275	33	293	75	290	56
PVA	273	28	–	–	–	–

It is seen from the table that the surface phonon frequencies much more strongly depend on the Raman excitation conditions than on the nanoparticle size or the host media type. However, the observed dependence cannot be unambiguously related to the resonance behaviour of the surface phonons in semiconductor nanoparticles. First of all, the observed decrease of the surface-to-LO phonon intensity ratio with the excitation wavelength decrease can originate from the LO phonon resonant enhancement at the Raman excitation energy approaching the HOMO–LUMO transition energy. Other factors, e. g. frequency dependence of the host medium dielectric response, can also contribute to the observed dependence. Besides, possible systematic errors in the extraction of the surface phonon contribution from the measured Raman spectra cannot be excluded: one should also keep in mind TO phonons as well as two-phonon excitations which can also contribute to the Raman scattering in this frequency range. Note that a similar situation was reported for CdSe [65]. Hence, the host medium effect on the surface phonon characteristics of CdS nanoparticles in dielectric matrices still requires further experimental studies.

4. Conclusions

CdS nanoparticles in different organic polymer media (gelatin, polyacrylamide, polyvinyl alcohol) were prepared from aqueous solutions at relatively mild conditions. Optical spectroscopic measurements (absorption, photoluminescence, Raman scattering) enabled us to estimate the average nanoparticle size and confirmed their good optical quality. The effects of the excessive Na_2S concentration and the synthesis temperature upon the CdS nanoparticle size were discussed.

Raman scattering spectra of CdS nanoparticles embedded in organic media have shown a distinct effect of phonon confinement and scattering by surface phonons, revealed in the LO phonon peak downward shift and asymmetric broadening. The effect of the host media type

on the surface phonon parameters appeared to be much smaller than the effect of the Raman resonance conditions.

Acknowledgements

Yu.M. Azhniuk is grateful to Deutsche Forschungsgemeinschaft for the financial support for his research at Chemnitz University of Technology where the Raman scattering studies were carried out. V.M.Dzhagan is obliged to Alexander von Humboldt foundation for the support of his research at Chemnitz University of Technology.

References

- [1] U. Woggon, Optical Properties of Semiconductor Quantum Dots, Springer, Berlin (1996).
- [2] C. B. Murray, C. R. Kagan, M. G. Bawendi, Ann. Rev. Mat. Sci. **30**, 545 (2000).
- [3] H. S. Nalwa (Ed.), Nanostructured Materials and Nanotechnology, Academic Press, San Diego (2000).
- [4] X. Michalet, F. Pinaud, T.D. Lacoste, M. Dahan, M.P. Bruchez, A.P. Alivisatos, Sh. Weiss, Single Mol. **4**, 261 (2001).
- [5] G. Schmid (Ed.), Nanocrystals: From Theory to Application, Wiley-VCH, Weinheim (2004).
- [6] C. Klingshirn, Landolt-Börnstein – Group III Condensed Matter, Optical Properties. Part 2 Volume 34C2, Springer, Berlin (2004)
- [7] A. Fu, W. Gu, C. Larabell, A.P. Alivisatos, Current Opinion Neurobiology **15**, 568 (2005).
- [8] R.C. Somers, M.G. Bawendi, D.G. Nocera. Chem. Soc. Rev. **36**, 579 (2007).
- [9] G.Z. Wang, W. Chen, C.H. Liang, Y. W. Wang, G. W. Wang, L. D. Zhang, Inorg. Chem. Commun. **4**, 208 (2001).
- [10] B. Liu, G. Q. Xu, L. M. Gan, C.H. Chew, W. S. Li, Z. X. Shen, J. Appl. Phys. **89**, 1059 (2001).
- [11] T. Hirai, T. Saito, I. Komasa, J. Phys. Chem. B **105**, 9711 (2001).
- [12] P. Nandakumar, C. Vijayan, Y. V. G. S. Murthi, J. Appl. Phys. **91**, 1509 (2002).
- [13] Y. Chen, X. Ji, Qi Sun, S. Jiang, B. Jiang, J. Non-Cryst. Sol. **311**, 314 (2002).
- [14] Ch. Barglik-Chory, D. Buchold, M. Schmitt, W. Kiefer, C. Heske, C. Kumpf, O. Fuchs, L. Weinhardt, A. Stahl, E. Umbach, M. Lentze, J. Geurts, G. Müller, Chem. Phys. Lett. **379**, 443 (2003).
- [15] S. F. Wuister, A. Meijerink, J. Luminesc. **105**, 35 (2003).
- [16] S. Kuwabata, K. Ueda-Sarson, T. Torimoto, Chem. Lett. **33**, 1344 (2004).
- [17] K. Kang, K. Daneshvar, J. Appl. Phys. **95**, 646 (2004).
- [18] P.K.Khanna, R.R. Gokhale, V.V.V.S. Subbarao, N. Singh, K.-W. Jun, B.K. Das, Mater. Chem. Phys. **94**, 454 (2005).

- [19] Y.-C. Chu, C.-C. Wang, C.-Y. Chen, *Nanotechnol.* **16**, 58 (2005).
- [20] M. Marandi, N. Taghavinia, A. Irajizad, S. M. Mahdavi, *Nanotechnol.* **16**, 334 (2005).
- [21] A. Merkoçi, S. Marýn, M. T. Castañeda, M. Pumera, J. Ros, S. Alegret, *Nanotechnol.* **17**, 2553 (2006).
- [22] P. Rodríguez, N. Muñoz-Aguirre, E. San-Martin Martínez, G. Gonzalez, O. Zelaya, J. Mendoza, *App. Surf. Sci.* **255**, 740 (2008).
- [23] J. Lee, V.K. Sundar, J.R. Heine, M.G. Bawendi, K.F. Jensen, *Adv. Mater.* **12**, 1102 (2000).
- [24] Sh.R. Bigham, J.L. Coffey, *J. Cluster Sci.* **11**, 359 (2000).
- [25] J.R. Lakowicz, I. Gryczynski, Z. Gryczynski, K. Nowaczyk, C. J. Murphy, *Analyt. Biochem.* **280**, 128 (2000).
- [26] M.J. Meziani, P. Pathak, B.A. Harruff, R. Hurezeanu, Y.-P. Sun, *Langmuir* **21**, 2008 (2005).
- [27] M. D. Fischbein, M. Drndic, *Appl. Phys. Lett.* **86**, 193106 (2005).
- [28] A. E. Raevskaya, A. L. Stroyuk, S. Ya. Kuchmiy, *Theoret. Experim. Chem.* **39**, 153 (2003).
- [29] A. E. Raevskaya, A. L. Stroyuk, S. Ya. Kuchmiy, *J. Nanoparticle Res.* **6**, 149 (2004).
- [30] Yu.M. Azhniuk, V.V. Lopushansky, A.V. Gomonnai, V.O. Yuhymchuk, I.I. Turok, Ya.I. Studenyak, *J. Phys. Chem. Sol.* **69**, 139 (2008).
- [31] W.W. Yu, L. Qu, W. Guo, X. Peng, *Chem. Mater.* **15**, 2854 (2003).
- [32] M. Nirmal, D.J. Norris, M. Kuno, M.G. Bawendi, A.L. Efros, M. Rosen, *Phys. Rev. Lett.* **75**, 3728 (1995).
- [33] D. Valerini, A. Creti, M. Lomascolo, L. Manna, R. Cingolani, M. Anni, *Phys. Rev. B* **71**, 235409 (2005).
- [34] Z. Yu, J. Li, D.B. O'Connor, L.-W. Wang, P.F. Barbara, *J. Phys. Chem. B* **107**, 5670 (2003).
- [35] T.J. Liptay, L.F. Marshall, P.S. Rao, R.J. Ram, M.G. Bawendi, *Phys. Rev. B* **76**, 155314 (2007).
- [36] A.L. Stroyuk, V.M. Dzhagan, D.R.T. Zahn, C. von Borczyskowski, *Theor. and Experim. Chem.* **43**, 297 (2007).
- [37] B. Tell, T.C. Damen, S.P.S. Porto, *Phys. Rev.* **144**, 771 (1966).
- [38] A. Roy, A.K. Sood, *Phys. Rev. B* **53**, 12127 (1996).
- [39] A. Ingale, K.C. Rustagi, *Phys. Rev. B* **58**, 7197 (1998).
- [40] A.V. Gomonnai, Yu.M. Azhniuk, V.O. Yuhymchuk, M. Kranjčec, V.V. Lopushansky, *Phys. Status Solidi (b)* **239**, 490 (2003).
- [41] A.K. Arora, M. Rajalakshmi, T.R. Ravindran, V. Sivasubramanian, *J. Raman Spectrosc.* **38**, 604 (2007).
- [42] A.G. Rolo, M.I. Vasilevskiy, *J. Raman Spectrosc.* **38**, 618 (2007).
- [43] P. M. Fauchet, I. H. Campbell, *Critical Reviews in Solid State and Materials Sciences* **14**, S79 (1988).
- [44] M. Nusimovici, J. L. Birman, *Phys. Rev.* **156**, 925 (1967).
- [45] P. Nandakumar, C. Vijayan, M. Rajalakshmi, A.K. Arora, Y. Murti, *Physica E* **11**, 377 (2001).
- [46] V. Sivasubramanian, A.K. Arora, M. Premila, C.S. Sundar, V.S. Sastry, *Physica E* **31**, 93 (2006).
- [47] L. Zeiri, I. Patla, S. Acharya, Y. Golan, S. Efrima, *J. Phys. Chem. C* **111**, 11843 (2007).
- [48] R.R. Prabhu, M. Abdul Khadar, *Bull. Mater. Sci.* **31**, 511 (2008).
- [49] A. Abdi, L.V. Titova, L.M. Smith, H.E. Jackson, J.M. Yarrison-Rice, J.L. Lensch, L.J. Lauhon, *Appl. Phys. Lett.* **88**, 043118 (2006).
- [50] X.-P. Shen, A.-H. Yuan, F. Wang, X. Xu, *Sol. St. Commun.* **133**, 19 (2005).
- [51] A.F.G. Monte, N.O. Dantas, P.C. Morais, D. Rabello, *Bras. J. Phys.* **36**, 427 (2006).
- [52] M.I. Vasilevskiy, A.G. Rolo, M.J.M. Gomes, O.V. Vikhrova, C. Ricolleau, *J. Phys.: Condens. Matter* **13**, 3491 (2001).
- [53] T. Komatsu, H. Mohri, M. Ohno, K. Matusita, *J. Matr. Sci. Lett.* **11**, 324 (1992).
- [54] J.J. Shiang, S.H. Risbud, A.P. Alivisatos, *J. Chem. Phys.* **98**, 8432 (1993).
- [55] H. Yükselici, P.D. Persans, T.M. Hayes, *Phys. Rev. B* **52**, 11763 (1995).
- [56] G. Scamarcio, M. Lugara, D. Manno, *Phys. Rev. B* **45**, 13792 (1992).
- [57] K.K. Nanda, S.N. Sarangi, S.N. Sahu, S.K. Deb, S.N. Bebera, *Physica B* **262**, 31 (1999).
- [58] V.S. Shusta, A.G. Slivka, O.O. Gomonnai, Yu. M. Azhniuk, V. V. Lopushansky, *J. Phys.: Conf. Ser.* **121**, 162001 (2008).
- [59] Yu. M. Azhniuk, A. G. Milekhin, A. V. Gomonnai, V. V. Lopushansky, V. O. Yuhymchuk, S. Schulze, E. I. Zenkevich, D. R. T. Zahn, *J. Phys.: Condens. Matter* **16**, 9069 (2004).
- [60] C. Trallero-Giner, *Phys. Stat. Sol. (b)* **241**, 572 (2004).
- [61] W. Xu, Y. Liao, D.L. Akins, *J. Chem. Phys. B* **106**, 11127 (2002).
- [62] I.-H. Choi, P.Y. Yu, *Phys. Stat. Sol. (b)* **242**, 1610 (2005).
- [63] R. Ruppin, *J. Phys. C: Solid State Phys.* **8**, 1969 (1975).
- [64] J. Pan, X. Xu, S. Ding, J. Pen, *J. Luminesc.* **45**, 45 (1990).
- [65] Yu. M. Azhniuk, Yu.I. Hutyk, V. V. Lopushansky, A. E. Raevskaya, A. L. Stroyuk, S. Ya. Kuchmiy, A.V. Gomonnai, D. R. T. Zahn, *J. Phys.: Conf. Ser.* **79**, 012017 (2007).

*Corresponding author: yu.azhniuk@gmail.com